

# Briefing Space Weather

2022/05/09

## 1 Sun

### 1.1 Responsible: Name

05/02 – Fast ( $=< 500$  km/s) wind stream; 4 CME c.h.c. toward the Earth;  
05/03 – 1 M1, 1 X1 and radio blackout ; Fast ( $=< 450$  km/s) wind stream; 8 CME c.h.c. toward the Earth;  
05/04 – 2 M5+ flares, 3 M1 and radio blackout; No fast wind stream; 8 CME c.h.c. toward the Earth;  
05/05 – 2 M1 flares; No fast wind stream; 5 CME c.h.c. toward the Earth;  
05/06 – No fast wind stream; 5 CME c.h.c. toward the Earth;  
05/07 – No fast wind stream; 2 CME c.h.c. toward the Earth;  
05/08 – No fast wind stream; 4 CME c.h.c. toward the Earth;  
05/09 – No fast wind stream; 1 CME c.h.c. toward the Earth;  
Prev.: No fast wind up to May 12; for the next 2 days relatively low (30% M, 5% X) probability of M / X flares; also,  
occasionally other CME can present component toward the Earth.  
c.h.c. – can have a component

## 2 Sun

### 2.1 Responsible: Name

- WSA-ENLIL (CME 2022-05-03T18:12Z)
  - The simulation results indicate that the flank of CME will reach the DSCOVR mission between 2022-05-08T01:00Z and 2022-05-08T15:00Z.
- WSA-ENLIL (CME 2022-04-27T08:48Z, 2022-04-27T14:53Z)
  - The simulation indicates that the Coronal Mass Ejections' flanks will reach the DSCOVR mission between 2022-05-11T04:00Z and 2022-05-11T18:00Z.

Buracos coronais (SPoCA : Spatial Possibilistic Clustering Algorithm):

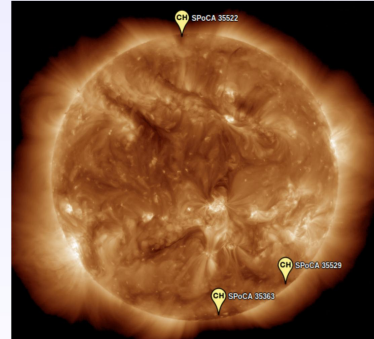
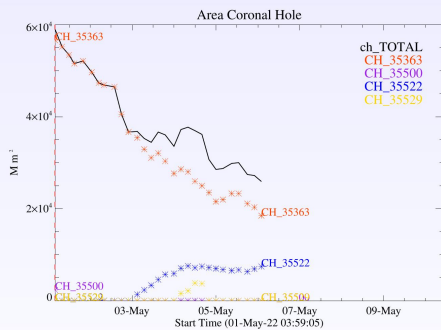
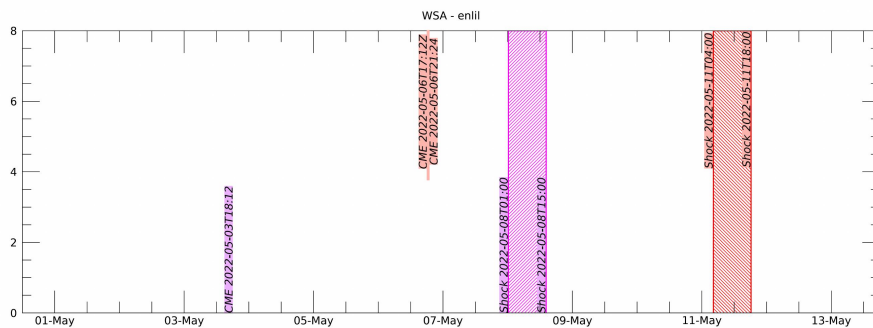


**Figura:** A linha em preto mostra o resultado da soma das áreas para cada intervalo da detecção realizado pelo SPOCA entre os dias 02 e 07 de maio de 2022

Sobre a imagem em 193 Å do Sol estão destacados os Buracos coronais observados pelo SPOCA por volta das 12:00 UT do dia 04 de maio de 2022.

A set of small, light-blue navigation icons typically found in Beamer presentations, including symbols for back, forward, search, and table of contents.

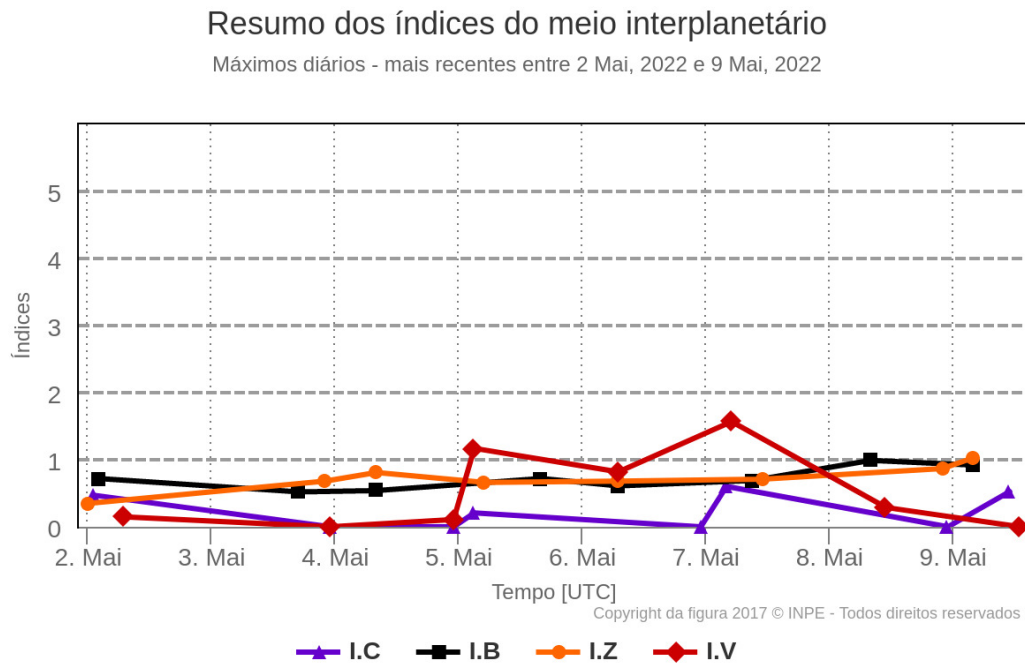
WSA - ENLIL SPOCA



A set of small, light-blue navigation icons typically found in presentation software like Beamer. They include symbols for back, forward, search, and table of contents.

### 3 Interplanetary Medium

#### 3.1 Responsible: Name



- The interplanetary medium region in the last week showed a low level of plasma perturbations due to the possible interaction of CME and HSS-like structures identified by the DISCOVERY satellite in the interplanetary medium.
- The modulus of the component of the interplanetary magnetic field showed 1 maximum peak : 08/May at 08:30 of 7.9 nT.
- The BxBy components showed variations in the analyzed period, both remaining oscillating within the [+5.5, -7.5] nT interval.
- The bz field component showed fluctuations with a positive value of 2.61 nT on May 09 at 07:30 and a negative value of -5.11 nT at 04:30 UT on May 09. On average, the Bz component oscillated mostly negative. Conditions favorable to the emergence of geomagnetic disturbances.
- The solar wind density oscillated mostly below 5 p/cm<sup>3</sup> during the analyzed period with a maximum peak on May 9 at 11:30 am of 16 p/cm<sup>3</sup>.
- The solar wind speed had oscillated mostly below 400 km/s throughout the presenting period.
- The magnetopause position was oscillating on average above the typical 10 Re position.

## 4 Radiation Belts

### 4.1 Responsible: Name

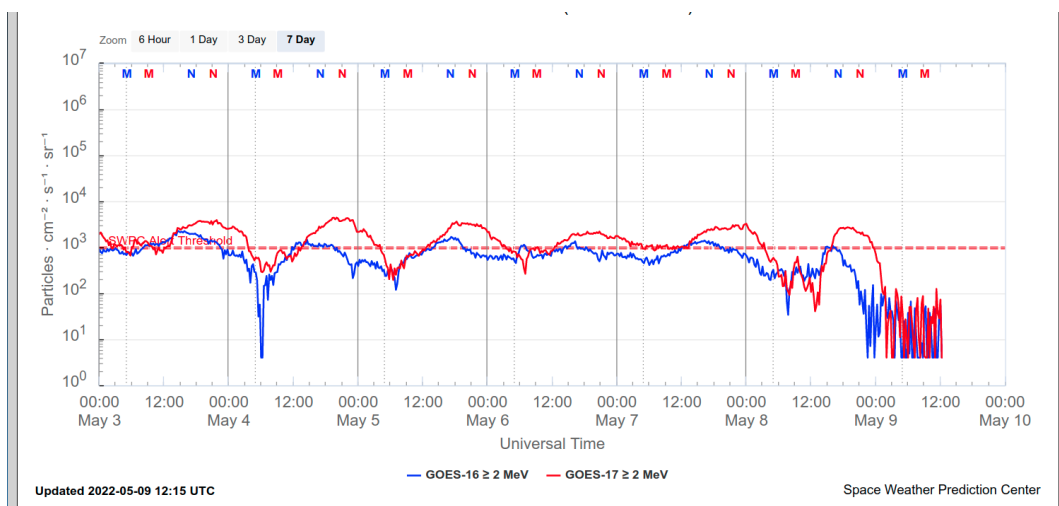


Figura 1: High-energy electron flux ( $\geq 2$  MeV) obtained from GOES-16 and GOES-17 satellite. Source

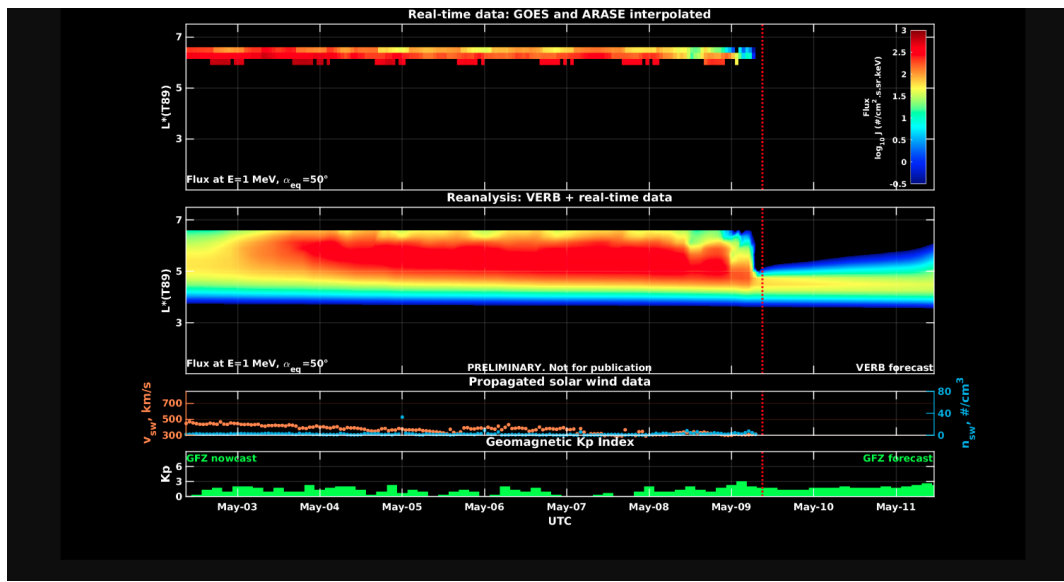


Figura 2: high-energy electron flux data (real-time and interpolated) obtained from ARASE, GOES-16, GOES-17 satellites. Reanalysis's data from VERB code and interpolated electron flux. Solar wind velocity and proton density data from ACE satellite. Source

High-energy electron flux ( $\geq 2$  MeV) in the outer boundary of the outer radiation belt obtained from geostationary satellite data GOES-16 and GOES-17 (Figure 1) is stable around the threshold 103 particles/(cm<sup>2</sup> sr) throughout the week of analysis. Three electron flux decreases were observed on May 4th, 8th, and 9th, respectively. The first decrease is considerably rapid, returning to the threshold of 103 particles/(cm<sup>2</sup> sr). The second decrease reaches approximately 1 order of magnitude and persists for more than 9n hours. The third electron flux decrease reaches approximately 2 orders of magnitude and persists until the last record.

The GOES-16, GOES-17, and Arase satellite data are analyzed and interpolated to observe the high-energy electron flux variability (1 MeV) in the outer radiation belt (Figure 2). Additionally, the VERB code rebuilds this electron considering the Ultra Low Frequency (ULF) waves' radial diffusion. The simulation (VERB code) shows that the first electron flux decrease occurs only at the outer boundary

of the outer radiation belt, the second reaches L-shell = 6.0, and the third reaches L-shell – 5.0. These electron flux variabilities occurred concomitantly with the arrival of solar wind structures and ULF wave activities. However, it is important to point out that the data from the ARASE satellite are not available for the week under analysis to confirm the L-shell level of these electron flux variabilities.

## 5 ULF Waves

### 5.1 Responsible: Name

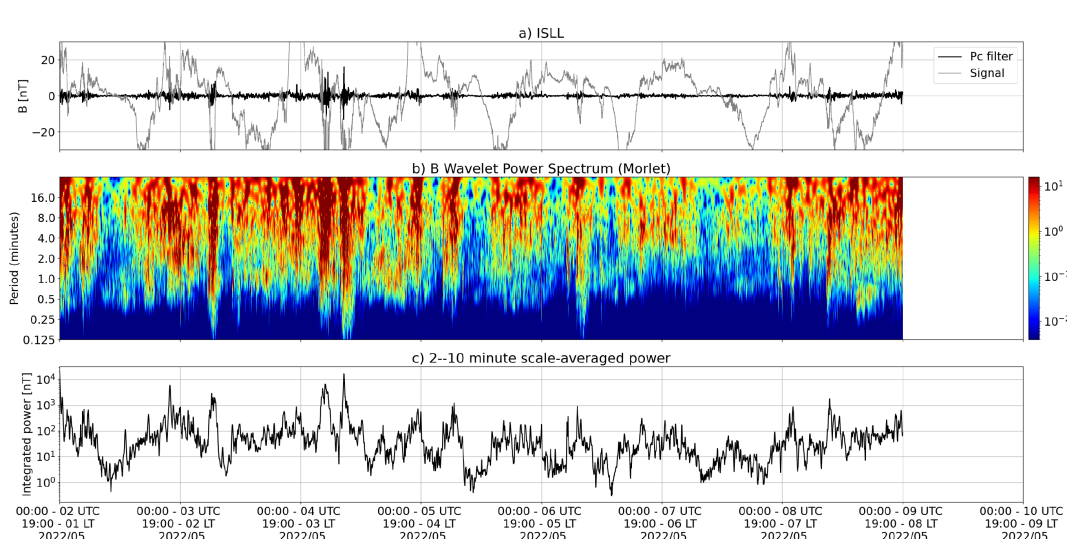


Figura 3: a) signal of the total magnetic field measured in the ISLL Station of the CARISMA network in gray, together with the fluctuation in the range of  $Pc5$  in black. b) Wavelet power spectrum of the filtered signal. c) Average spectral power in the ranges from 2 to 10 minutes (ULF waves).

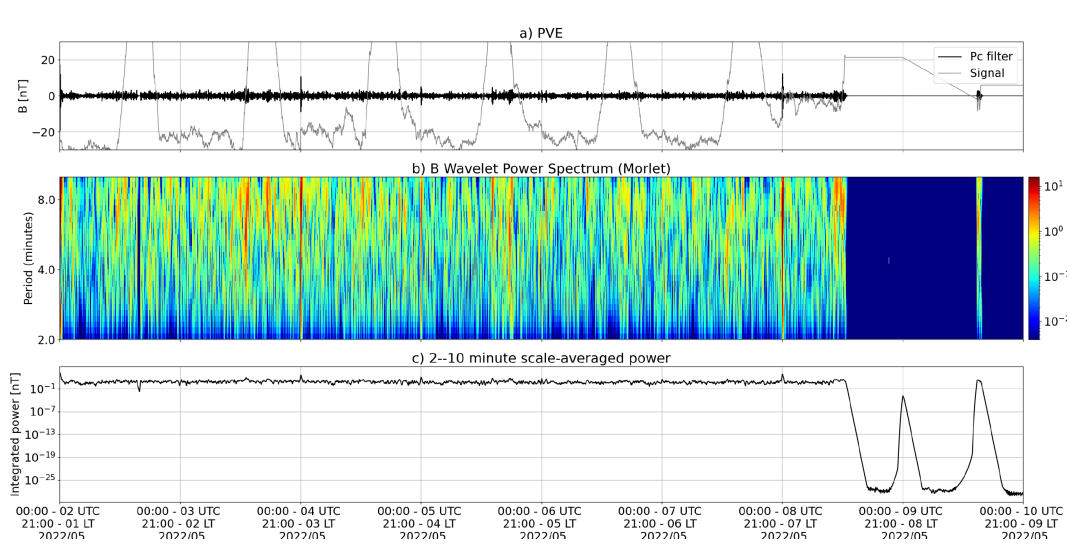


Figura 4: a) signal of the total magnetic field measured in the EMBRACE network in gray, together with the fluctuation in the range of  $Pc5$  in black. b) Wavelet power spectrum of the filtered signal. c) Average spectral power in the ranges from 2 to 10 minutes (ULF waves).

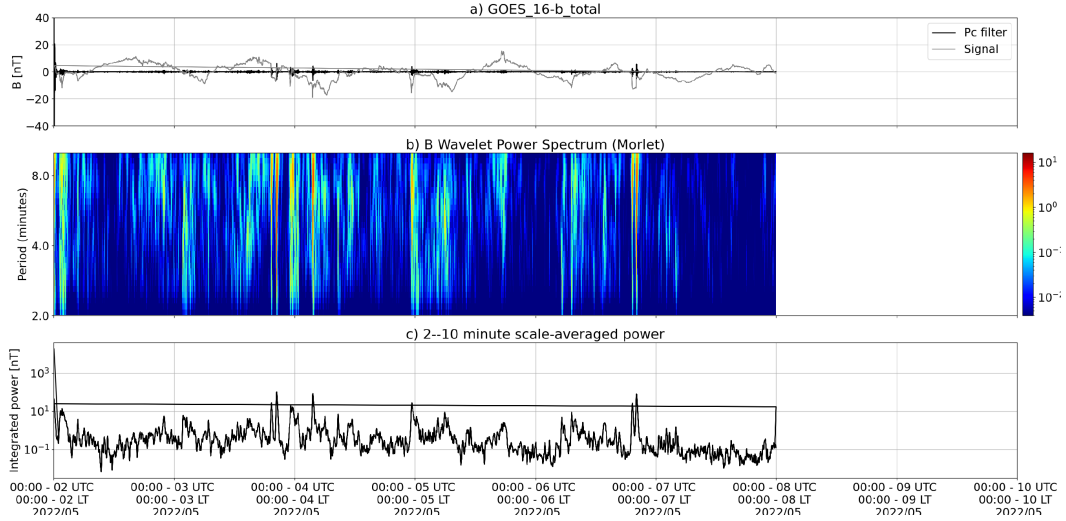
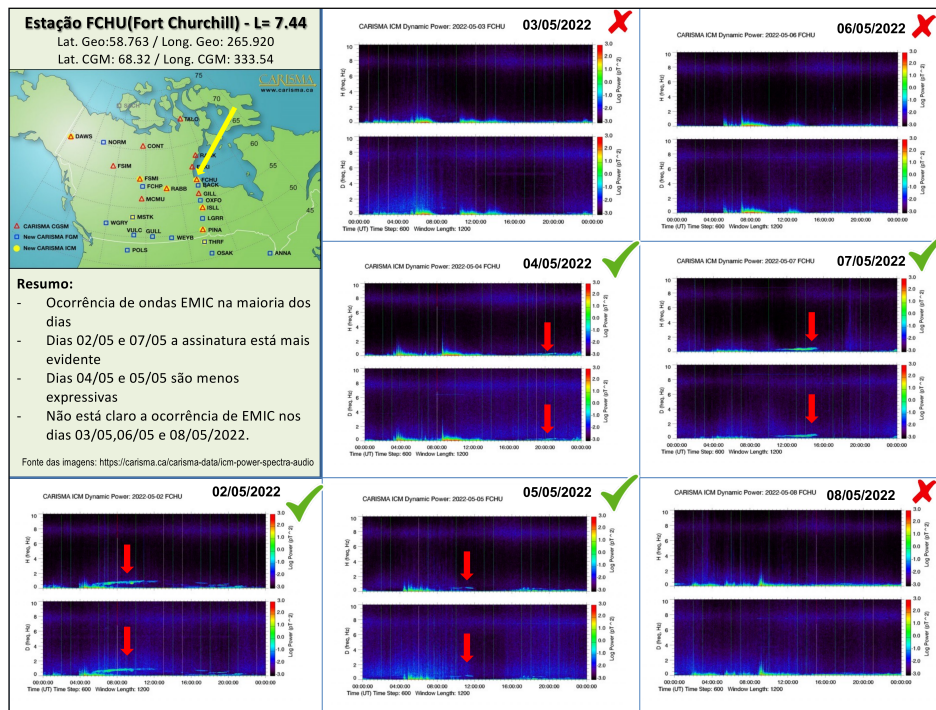


Figura 5: a) signal of the total magnetic field measured by the GOES 16 satellite, together with the fluctuation in the range of  $\text{Pc}5$  in black. b) Wavelet power spectrum of the filtered signal. c) Average spectral power in the ranges from 2 to 10 minutes (ULF waves).

The ULF wave activity shows an increase in power from the 3rd of May in the form of irregular and short-duration pulsations, detected from high latitudes to the magnetometers at low latitudes of the EMBRACE network (Figure 2, SMS), the same activity repeats on May 4th. The activity continues until the 7th of May with reduced power. On day 8, there is a further increase in spectral power, now with continuous characteristics, mainly at high latitudes. This period is possibly under the effect of a corrotant interaction region (CIR) and also periods with an increase in the density of the solar wind and component of the magnetic field of the solar wind predominantly in the south direction. Summary 10/10 The ULF wave activity shows an increase in power from the 3rd of May in the form of irregular and short-duration pulsations, detected from high latitudes to the magnetometers at low latitudes of the EMBRACE network (Figure 2, SMS), the same activity repeats on May 4th. The activity continues until the 7th of May with reduced power. On day 8, there is a further increase in spectral power, now with continuous characteristics, mainly at high latitudes. This period is possibly under the effect of a corrotant interaction region (CIR) and also periods with an increase in the density of the solar wind and component of the magnetic field of the solar wind predominantly in the south direction.

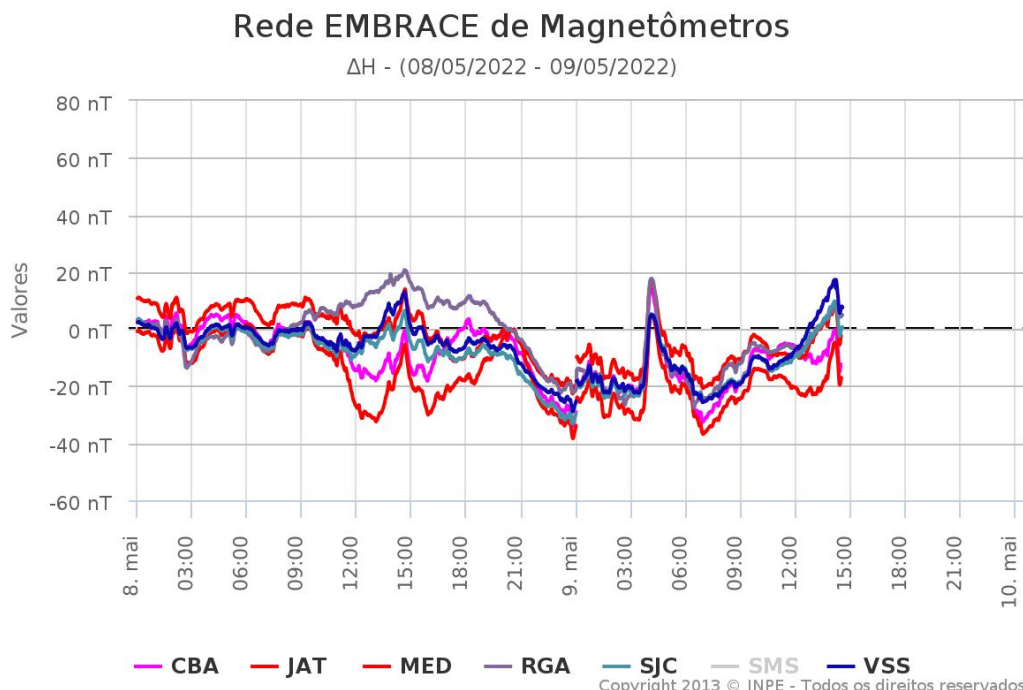
## 6 Ondas EMIC

### 6.1 Responsável: Name



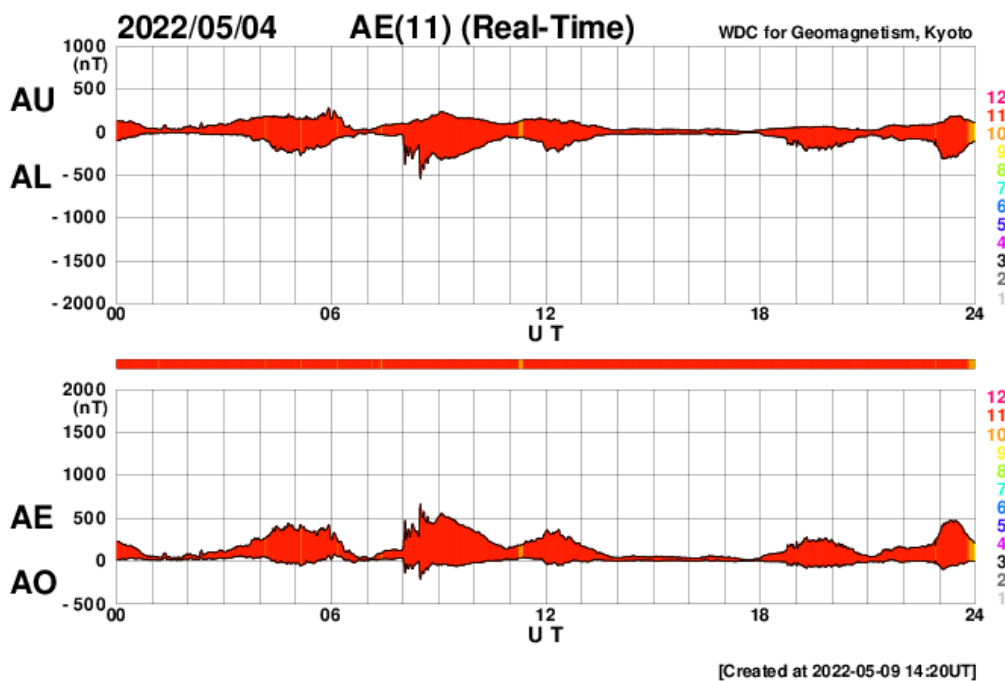
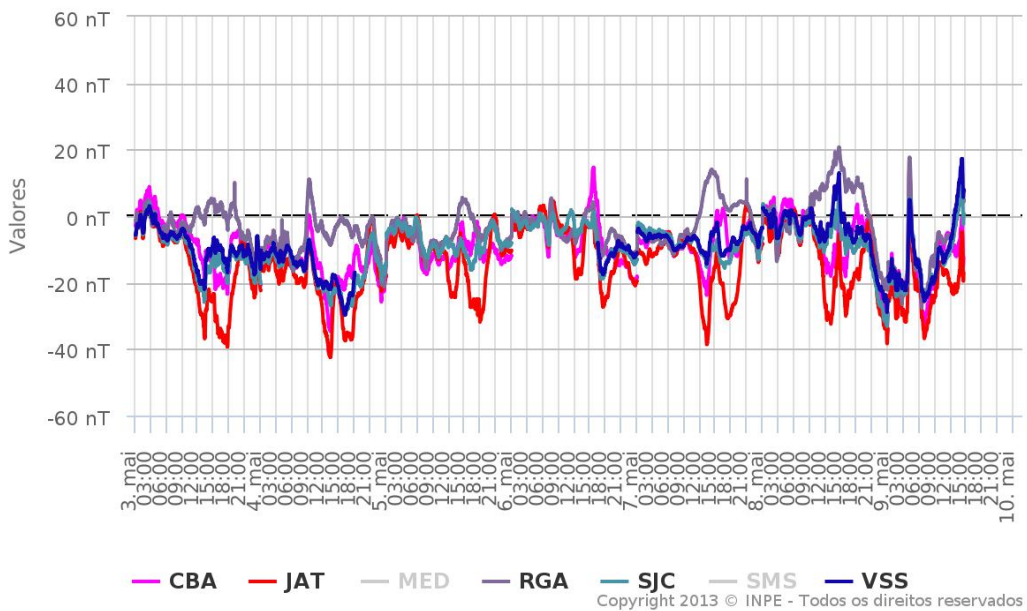
## 7 Geomagnetism

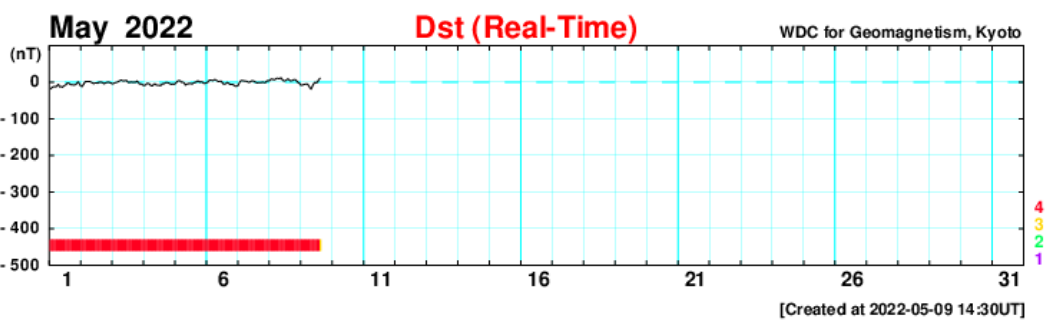
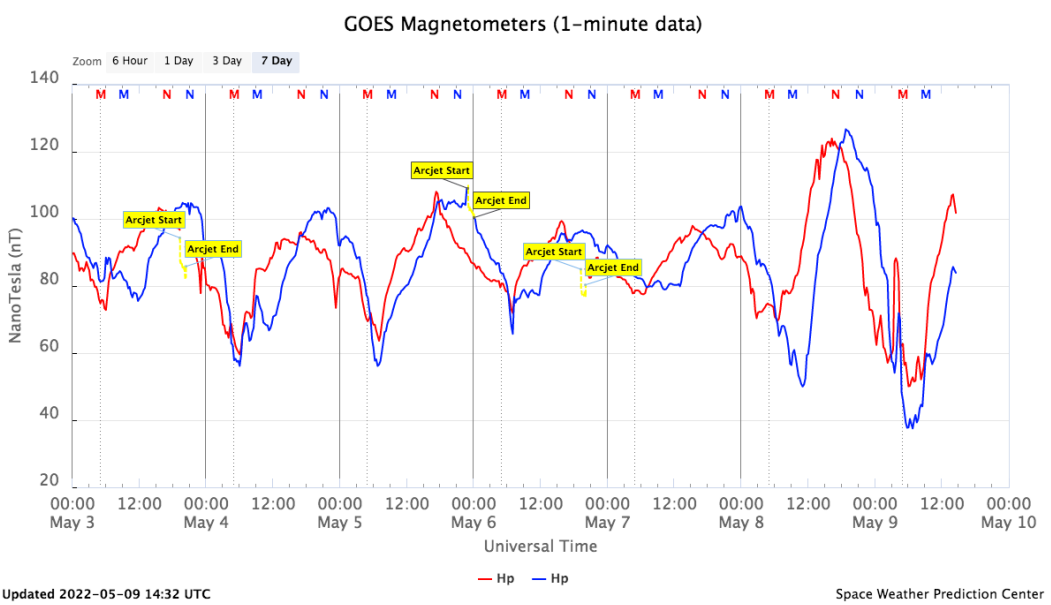
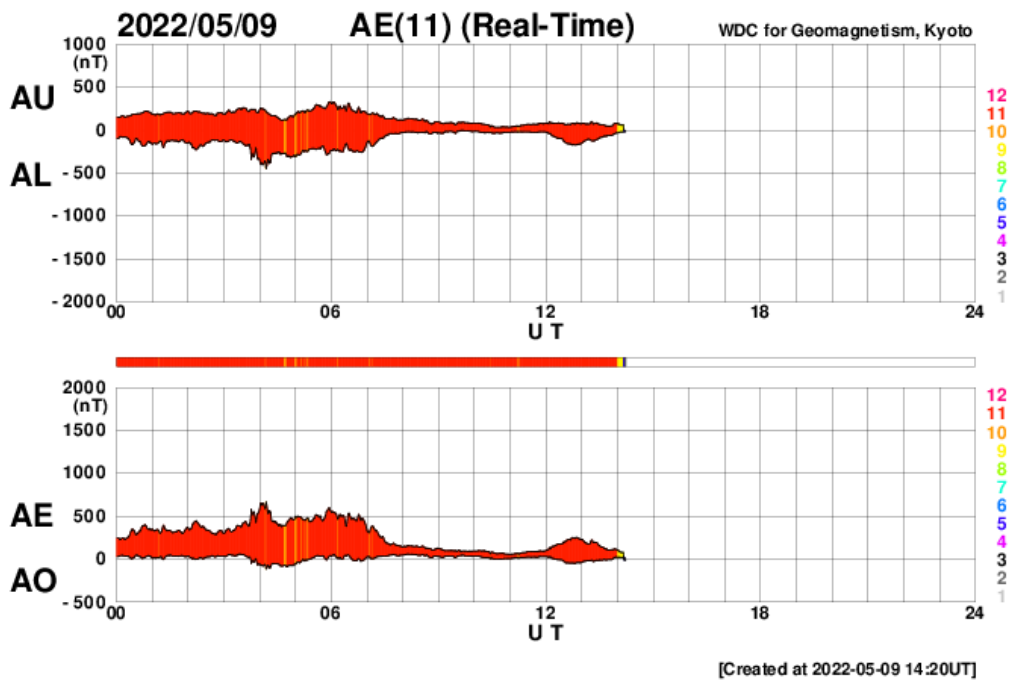
### 7.1 Responsible: Name

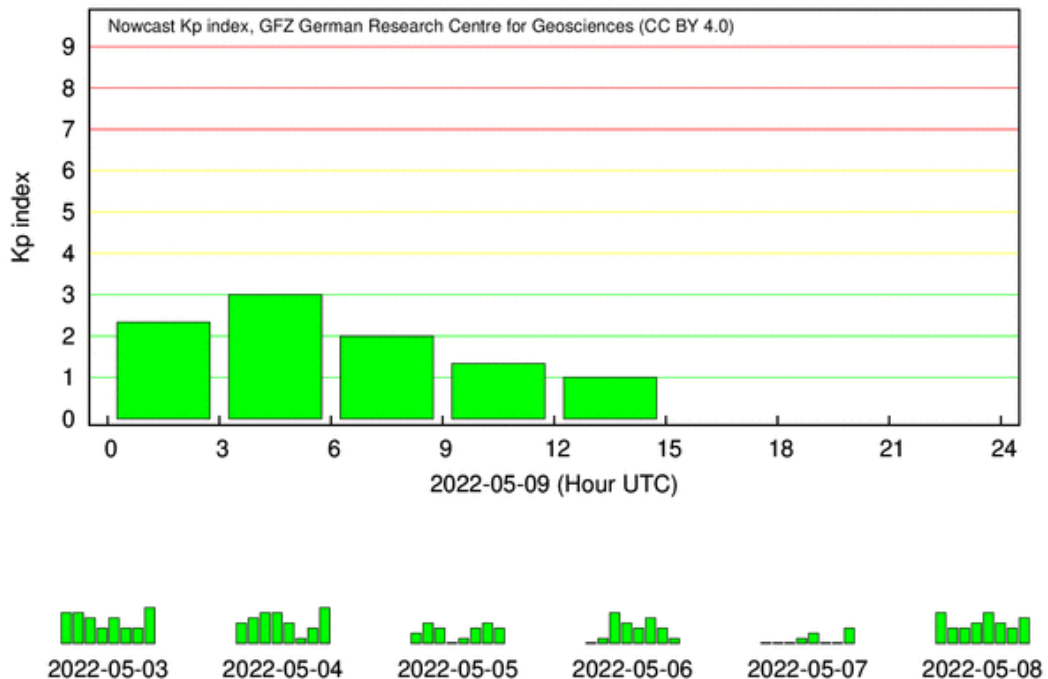


## Rede EMBRACE de Magnetômetros

ΔΗ - (03/05/2022 - 09/05/2022)







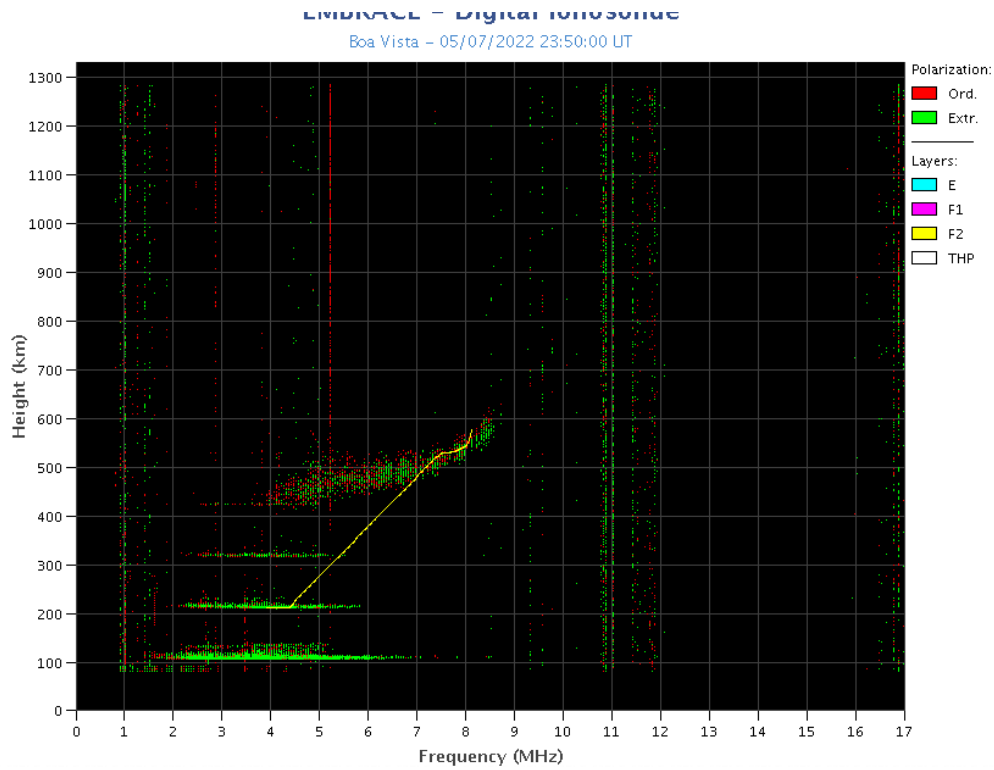
- Data from the Embrace magnetometer network showed instabilities throughout the period, with some events highlighted:
  - The highest H instabilities were registered on May 3, 8 and 9
  - Geomagnetic activity was unsettled, with the Dst index reaching around zero. The highest Kp of the week was 30.
  - The auroral activity was intensified on May 4 and 9.
  - Magnetic field measured in the orbit of the GOES satellite showed disturbances on May 09.

## 8 Ionosphere

### 8.1 Responsible: Name

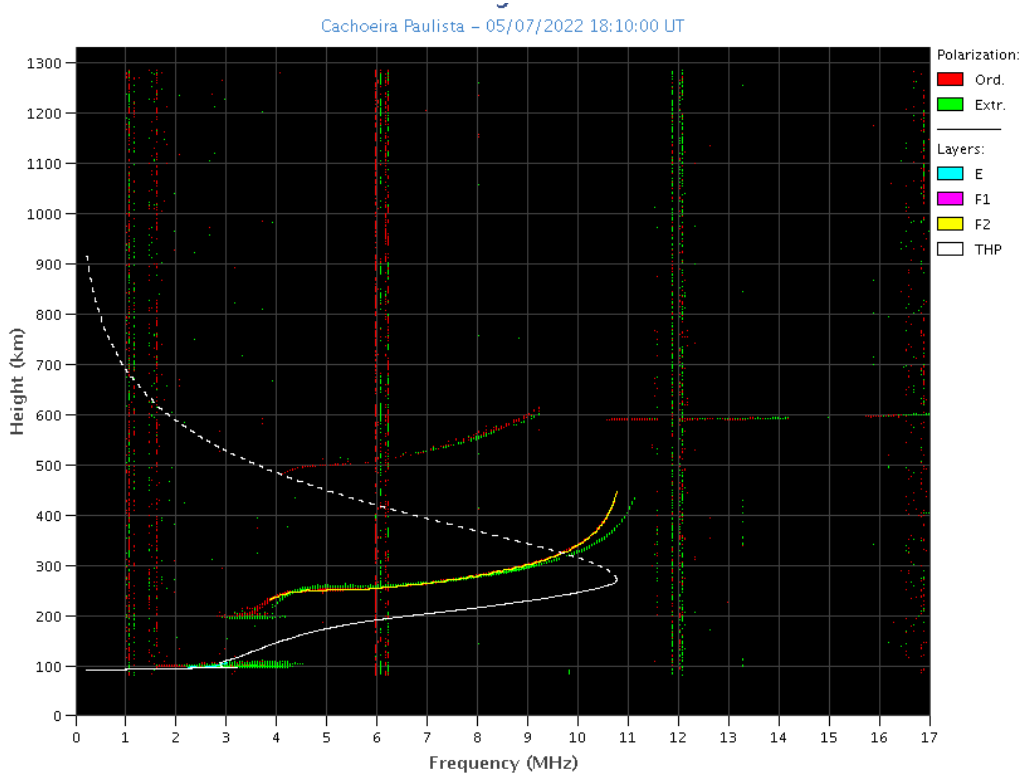
**Boa Vista:**

- There were spread F during all days in this week.
- The Es layers reached scale 4 on day 07.



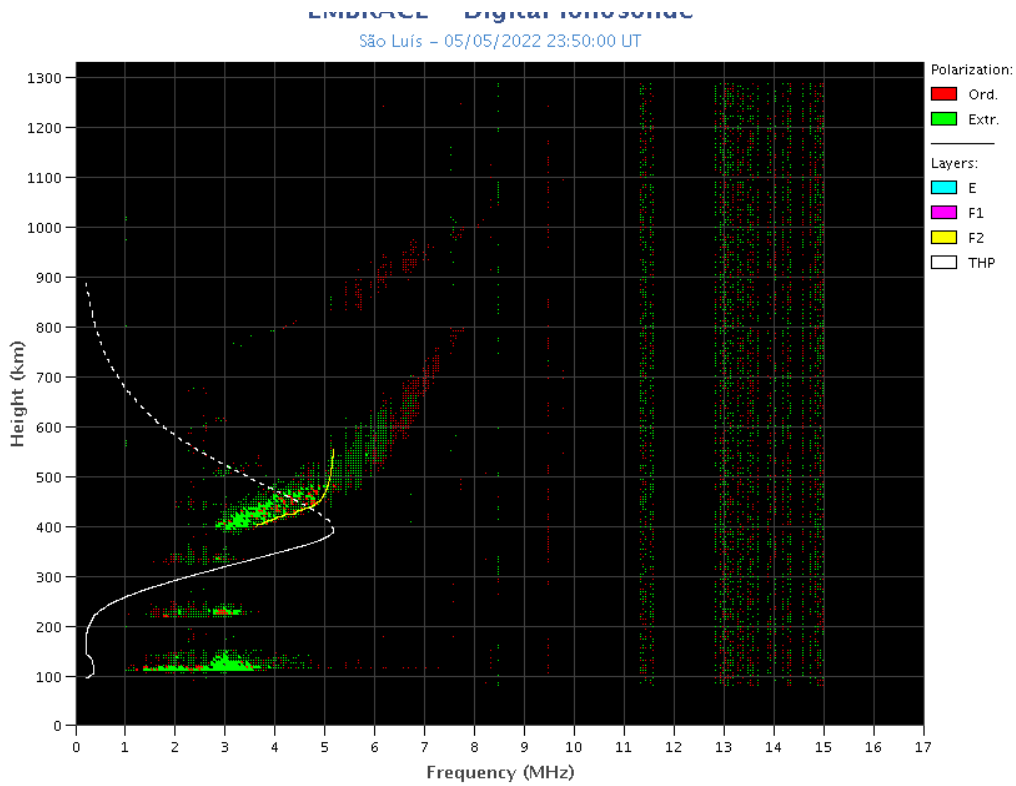
### Cachoeira Paulista:

- There were not spread F in this week.
- The Es layers reached scale 2 during this all week.



### São Luís:

- There were spread F during all days in this week.
- The Es layers reached scale 5 on day 05.



## 9 SCintilation

### 9.1 Responsible: Name

In this report on the S4 scintillation index, data from FRTZ in Fortaleza/CE, STSN in Sinop/MG, UFBA in Bahía/BA and SJCE in São José dos Campos/SP are presented. The S4 index tracks the presence of irregularities in the ionosphere having a spatial scale  $\sim 360$  m. The stations STSN, STNT and SJCE did not present relevant values of the S4 index throughout the week. In the FRTZ station, a case appeared with S4 values above 0.4. The most important was recorded in the morning of 04/25 (Figure 1, upper panel). In the lower panel of Figure 1, the affected satellites located to the northwest of the FRTZ appear. Ionograms at the same time and location show the typical spread in the main trace. This fact together with the position of satellites with S4 values  $> 0.15$  shown in the Figure 1 indicate the presence of an irregularity in the ionospheric plasma due to a typical plasma bubble at this time and at these latitudes close to the geomagnetic equator.

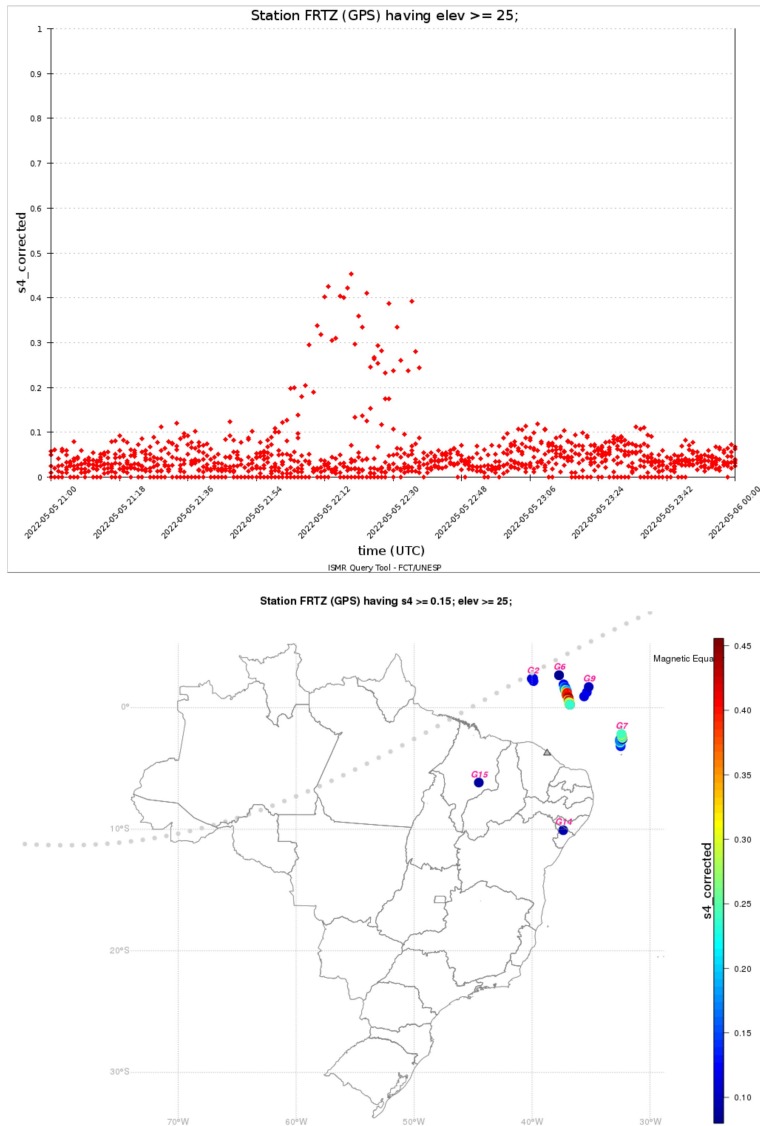


Figura 1: Valores do índice S4 correspondente à constelação GPS para a estação FRTZ no dia 5/05. Entre às 2100 e as 0000 UT (painel superior). No painel inferior o mapa dos valores do S4 > 0.15 para os satélites GPS com elevação > 25° no campo de visada do receptor da mesma estação do painel superior e para o mesmo intervalo de tempo.



## 10 All-Sky Imager

### 10.1 Responsible: Name

**All-Sky Imager EPBs Observation || May 01 - May 07, 2022**  
**Observações das EPBs por meio do imageador All-Sky -**  
**|| 01 - 07 maio, 2022**

Observatory Observatório	May 01 maio 01	May 02 maio 02	May 03 maio 03	May 04 maio 04	May 05 maio 05	May 06 maio 06	May 07 maio 07
CA	✓◐	✓●	✓●	✓◐	✓●	✓○	✓◐
BJL	✗	✗	✗	✗	✗	✗	✗
CP	✓◐	✗	✓◐	✓◐	✓◐	✓●	✗
SMS	✓●	✓●	✓●	✓●	✓○	✓◐	✓○
CA	São João do Cariri						
BJL	Bom Jesus da Lapa						
CP	Cachoeira Paulista						
SMS	São Martinho da Serra						
✓	Observation - Observação						
✗	No Observation - Sem Observação						
○	Clear sky - Céu limpo						
◐	Partly Cloudy - Parcialmente Nublado						
●	Cloudy - Nublado						
✳	Blur image - Desfocar Imagem						

- At the Sao Joao do Cariri observatory, a small plasma bubble structure was observed on the night of May 3-4. Besides, on the night of May 06- 07, a traveling ionospheric disturbances was observed propagating to the northeast.
- At the Bom de Jesus da Lapa observatory there was no observation due to technical problems.
- At the Cachoeira Paulista no plasma bubbles were observed during the entire week even though there were observation.
- Finally, at the observatory of Sao Martinho da Serra, no plasma bubble structures were observed during the entire week. 2

## TEC

- No plasma bubbles were observed during the entire period. As bubble sea- sonality is at the end, plasma bubbles have small spatial dimensions and they are difficult to observe on TEC maps. 3

## 11 ROTI

### 11.1 Responsible: Name

ROTI did not show significant variations related to ionospheric irregularities during the week. However, it is interesting to mention that some structures appear in the northern region of Brazil every day of the week. However, this region has low spatial coverage of GNSS receivers, and there are also the border's effects on the maps, causing an error propagation in this specific region.